AAPS PharmSciTech, Vol. 10, No. 1, March 2009 (© 2009)
DOI: 10.1208/s12249-009-9187-4

Research Article

Crystal Morphology Engineering of Pharmaceutical Solids: Tabletting Performance Enhancement

Sabiruddin Mirza,[1,5] Inna Miroshnyk,[1] Jyrki Heinämäki,[1] Osmo Antikainen,[1] Jukka Rantanen,[2] Pia Vuorela,[3] Heikki Vuorela,[4] and Jouko Yliruusi[1]

Received 29 August 2008; accepted 31 December 2008; published online 30 January 2009

Abstract. Crystal morphology engineering of a macrolide antibiotic, erythromycin A dihydrate, was investigated as a tool for tailoring tabletting performance of pharmaceutical solids. Crystal habit modification was induced by using a common pharmaceutical excipient, hydroxypropyl cellulose, as an additive during crystallization from solution. Observed morphology of the crystals was compared with the predicted Bravais–Friedel–Donnay–Harker morphology. An analysis of the molecular arrangements along the three dominant crystal faces [(002), (011), and (101)] was carried out using molecular simulation and thus the nature of the host–additive interactions was deduced. The crystals with modified habit showed improved compaction properties as compared with those of unmodified crystals. Overall, the results of this study proved that crystal morphology engineering is a valuable tool for enhancing tabletting properties of active pharmaceutical ingredients and thus of utmost practical value.

KEY WORDS: crystal engineering; crystal habit; erythromycin A dihydrate; hydroxypropyl cellulose; tabletting properties.

INTRODUCTION

The successful development and commercialization of an active pharmaceutical ingredient (API) require adequate processability, stability, and bioavailability (1). However, APIs with desired biological activities rarely exhibit adequate physical properties to meet all of the requirements. Crystal engineering, the design of molecular solids in the broadest sense (2,3), is gaining an increased interest within the pharmaceutical industry because it enables preparation of materials with tailored physical properties.

One persistent challenge in the development and manufacturing of APIs is poor tabletting performance (4,5). Crystal habit, or morphology, is a crucial attribute of powdered materials that affects the ease with which a pharmaceutical formulation can be pressed into a tablet. In particular, equidimensional crystals are usually preferred in the industry as they have better handling and processing characteristics such as flowability and compactability (6–8). Crystal morphology engineering is therefore a valuable tool to enhance processing properties of solid materials for a specific formulation.

Control of crystal morphology can be achieved by solvent selection (9–12) and/or tailor-made additives (13–15). In the context of pharmaceutical solids, the solvent-induced crystal habit modification approach is limited by the solvent toxicity and cost, crystallization efficiency, and the purity requirements of the final product. Hence, the use of additives as crystal habit modifiers of APIs is usually preferred. Furthermore, employing pharmaceutically accepted excipients as additives represents the most practical alternative for such a highly regulated industrial sector as the pharmaceutical industry.

This study therefore aims to (1) investigate crystallization in the presence of pharmaceutically accepted excipients as a tool for crystal morphology engineering of APIs and (2) evaluate compaction properties of the additive-modified crystals. Erythromycin A dihydrate (EMAD; Fig. 1a), a widely prescribed macrolide antibiotic possessing poor compaction properties, was selected as a model API, while hydroxypropyl cellulose (HPC; Fig. 1b) was chosen as a crystal habit modifier, based on the preliminary additive screening experiments in our laboratory.

[1] Division of Pharmaceutical Technology, Faculty of Pharmacy, University of Helsinki, P.O. Box 56, 00014, Helsinki, Finland.
[2] Department of Pharmaceutics and Analytical Chemistry, Faculty of Pharmaceutical Sciences, University of Copenhagen, Copenhagen, Denmark.
[3] Department of Biochemistry and Pharmacy, Åbo Akademi University, Turku, Finland.
[4] Division of Pharmaceutical Biology, Faculty of Pharmacy, University of Helsinki, Helsinki, Finland.
[5] To whom correspondence should be addressed. (e-mail: sabir.mirza@helsinki.fi, URL: http://www.pharmtech.helsinki.fi/english/front page.htm)

ABBREVIATIONS: EMAD, erythromycin A dehydrate; BFDH, Bravais–Friedel–Donnay–Harker; HPC, hydroxypropyl cellulose; DSC, differential scanning calorimetry; PXRD, powder X-ray diffraction; SEM, scanning electron microscope.

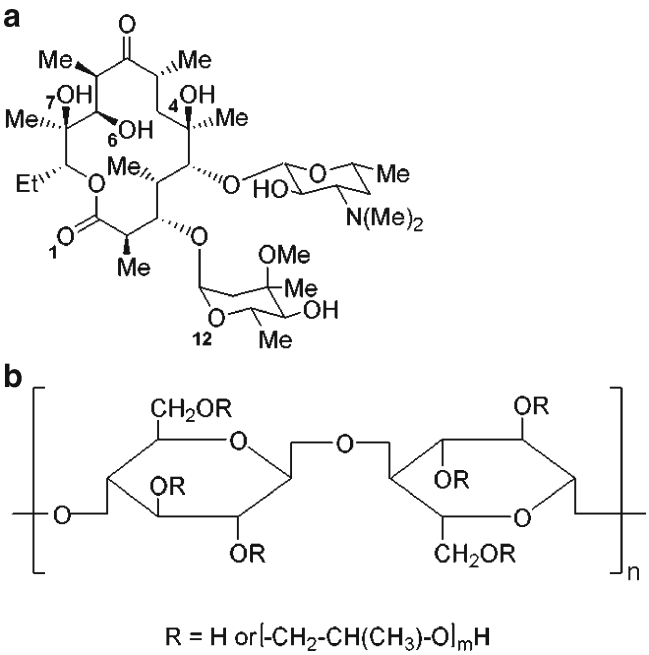

Fig. 1. Molecular structures for the model API, erythromycin A **a** and hydroxypropylmethylcellulose, a pharmaceutical excipient used as crystal habit modifier in this study **b**. The relevant oxygen atoms are numbered in panel **a**

MATERIALS AND METHODS

Materials

EMAD (MW=770 g/mol; Sandoz, Italy) was used as received. HPC (Fluka, Buchs, Switzerland) was used as additive. Ethanol of analytical grade and purified water (Ph. Eur.) were used as solvents.

Methods

Additive-Mediated Crystallization

The crystallizations ($n=3$) were carried out by precipitation technique at ambient temperature, as schematically shown in Fig. 2. Briefly, a saturated solution of the drug in ethanol was slowly poured into an aqueous solution of HPC of varying concentrations under constant stirring and the experiments were completed at solvent to antisolvent ratio of 1:9 (v/v). The solvent system that yields the desirable dihydrate form of the model API has been identified in our previous study (16). The additive concentrations in the crystallization medium studied were 0, 0.45, 2.25, or 4.5 wt. % (hereafter referred to as *reference*, *L crystals*, *M crystals*, *and H crystals*, respectively).

Physical Characterization of Solid Materials

Powder X-ray diffraction (PXRD) studies were done using a theta–theta diffractometer (D8 Advance, Bruker axs GmbH) fitted with a scintillation counter. The experiments were performed in symmetrical reflection mode using a CuKa radiation source (wavelength 1.54 Å) with Göbel Mirror bent gradient multilayer optics. Data points were collected between 5° and 40° 2θ with steps of 0.1° and a measuring time of 1 s per step.

A DuPont differential scanning calorimeter (Model 910S, TA Instruments Inc.) equipped with a data station (Thermal Analyst 2000, TA Instruments Inc.) was used to determine the differential scanning calorimetry (DSC) curves. The temperature was calibrated with benzophenone and indium (melting points at 48.0°C and 156.6°C, respectively). Enthalpy calibration of the DSC signal was performed with indium (10 mg, 99.999% pure, and heat of fusion 28.4 J g^{-1}). Samples were analyzed in open aluminum pans at a heating rate of 10°C min^{-1} under static air.

The water content of the samples was determined by Karl Fisher (KF) titration with a Mettler KF titrator (model DL35, Metler Toledo AG, Greifensee, Switzerland) using Hydranal Working Medium K Solvent and Hydranal Composite 5K Titrant. Samples (~150 mg) were accurately weighed and quickly transferred to a titration vessel to minimize the uptake of atmospheric moisture. The measurements were made in triplicate.

Scanning electron microscope (SEM) images were recorded with a Zeiss DSM-962 (Carl Zeiss, Oberkochen, Germany) scanning electron microscope at an acceleration voltage of 4–15 kV and were used to examine crystal morphology. Prior to the capturing, the samples were attached to double-sided carbon tape and coated with 20 nm platinum using an Agar sputter coater B7304 (Agar Scientific Ltd., Stansted, UK).

Analysis of the Drug Content

The content of erythromycin A was determined as the average of two high-performance liquid chromatography (HPLC) determinations according to the method described in the *European Pharmacopoeia* (fifth edition). The HPLC system consisted of a Waters 600E Multisolvent Delivery System, autosampler 717, and programmable photodiode

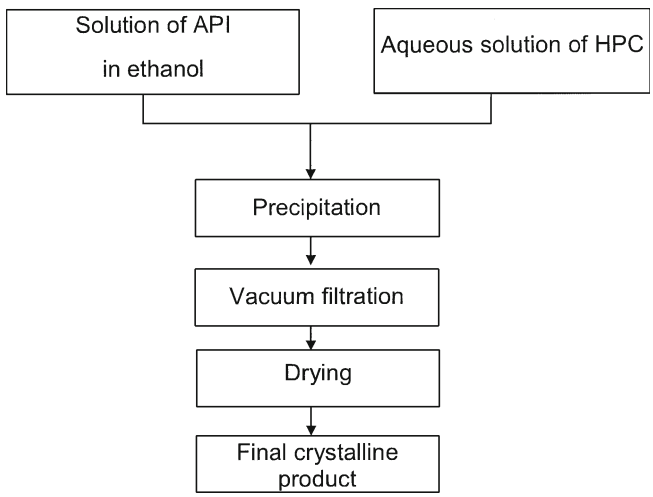

Fig. 2. A schematic representation of the crystallization process

array detection system 991 (Millipore, USA) coupled to a Nec Power Mate 386/25 personal computer (USA).

The amounts of the additive, A (%), possibly adsorbed by the crystal surfaces were estimated as follows:

$$A = 100 - \text{drug content}\,(\%) \tag{1}$$

Evaluating Powder Compaction Properties

Crystal compaction behavior was evaluated with an instrumented eccentric tablet machine (Korsch EK0, Erweka Apparatebau, Germany). For each experiment, the powder (250±10 mg) was manually poured into a die and compacted at compression pressures varying in the range from 2,800 to 6,300 N by using 9-mm-diameter flat-faced punches. Crushing strength of the tablets was measured using a tablet hardness tester (Erweka, Germany). In addition, the elasticity of the materials was evaluated in terms of elasticity factor, EF, calculated using the following equation:

$$\mathrm{EF} = \left(\frac{s_{\max} - s_{0\mathrm{d}}}{s_{\max} - s_0}\right)100\% \tag{2}$$

where $s_{\max}$ is the maximal upper punch displacement; s_0 is the upper punch displacement when force is noticed first; and $s_{0\mathrm{d}}$ is the upper punch displacement in the decompression phase when force has dropped to zero. The details of the procedure can be found elsewhere (17).

Simulation of Powder Diffraction Data and Molecular Modeling

The single crystal X-ray diffraction data for EMAD (18) (refcode: NAVTAF) were retrieved from the Cambridge Structural Database. The theoretical powder X-ray diffraction pattern was calculated, and the Miller index of each diffraction peak was assigned using the Diffraction-Crystal Module of Cerius (2). The theoretical growth form was computed by using molecular simulation software (Mercury, Cambridge Crystallographic Data Center, CCDC, Cambridge, UK, v. 1.5) according to the Bravais–Friedel–Donnay–Harker (BFDH) theory. The same software was used for crystal structure visualization.

RESULTS

Effect of Additive Concentration on the Crystal Morphology

The visual comparison of the observed crystal morphology on the SEM images (Fig. 3) revealed that the effect HPC exhibits on the crystal habit of EMAD is concentration dependent. The reference crystals (Fig. 3a) showed a range of shapes, from irregular to acicular and plate like. One explanation of such diverse morphology is fast crystal growth (most likely due to the high degree of supersaturation) that prevents the formation of fully developed crystals. On the contrary, the additive-treated crystals all exhibited characteristic morphology. Specifically, crystallization in the presence of 0.45 wt.% of HPC yielded plate-like crystals (Fig. 3b). Upon further increase in the polymer concentration to 2.25 and 4.5 wt.%, elongated plate-like crystals (Fig. 3c) were produced.

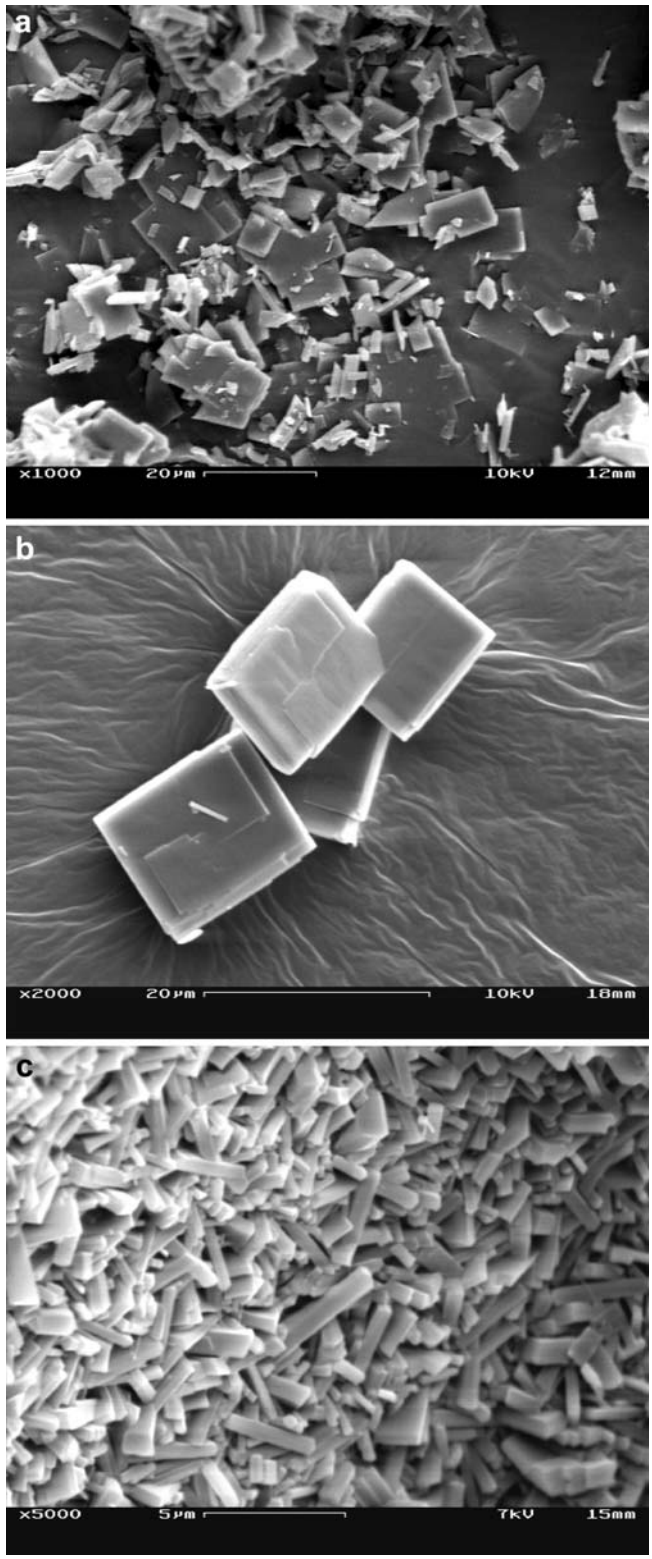

Fig. 3. SEM images of erythromycin A dihydrate crystals grown in the presence of various concentrations of HPC: **a** 0 (reference), **b** 0.45 (L crystals), and **c** 4.5 wt.% (H crystals)

Predicted Morphology of the EMAD Crystals

To better understand particular morphological effects with respect to the present crystallizing system, the predicted BFDH morphology of the EMAD crystal was visualized (Fig. 4a). Application of the BFDH theory is a quick approach for identifying the crystallographic forms {*hkl*} most likely to constitute a crystal habit. According to the BFDH theory, the relative growth rate of a face is inversely proportional to the interplanar spacing *d* and hence the most morphologically important faces of the crystal are those that have the biggest *d* values (19,20). In the case of EMAD, these planes are (002) (d=23.6 Å), (011) (d=9.4 Å), and (101) (d=9.0 Å), as determined by indexing the single crystal data. Consequently, the predicted shape of EMAD is plate like, slightly elongated along *b* direction, and bounded by faces (002), (011), and (101). In addition, small (110) faces appear as the boundary between the (011) and (101) crystal faces. The comparison of this model with the observed morphology of the crystals indicates that the morphology of L crystals (Fig. 4b) is in reasonable agreement with the BFDH model.

Solid-State Properties of the HPC-Modified Crystals

Additive-mediated crystallization is often employed to produce a desirable solid-state modification of the API (14,21,22) and thus can cause unwanted solid-phase transformations (23,24). Therefore, solid-state analysis was further performed to examine the effect of HPC on the physical form of the model API. Comparison of the computed PXRD pattern for EMAD and the experimental patterns (Fig. 5) revealed that, apart from intensity differences, which can be attributed to preferred orientation in the samples, there was an excellent correspondence between the peak angular positions. In addition, no amorphous halo was observed in the experimental PXRD patterns. Therefore, it can be concluded that no phase transition occurred during crystallization and all crystals represent phase-pure EMAD.

Further, the reflections associated with the dominant crystal faces were examined more closely. The reflection corresponding to the (002) crystal plane appears at around 3.7° 2θ and hence could not be detected with wide-angle PXRD. The diffraction peak associated with the (011) plane is poorly resolved due to its low relative intensity. The intensity of the diffraction peak corresponding to the (101) crystal plane in the patterns of M and H crystals was observed to slightly decrease as compared with that of L crystals or the

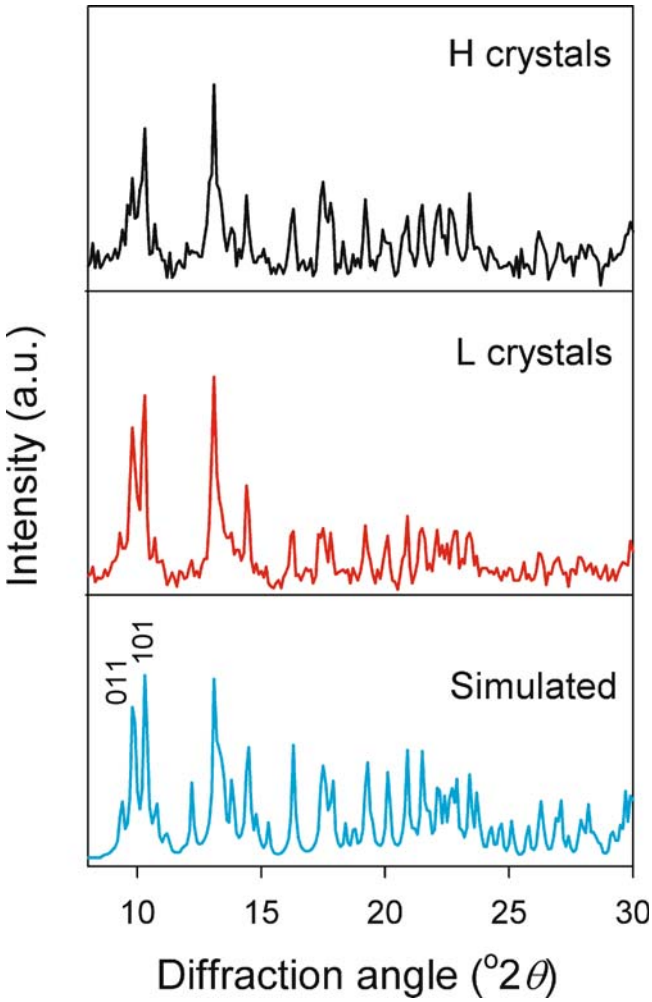

Fig. 5. Comparison of the experimental and simulated PXRD patterns of erythromycin A dihydrate

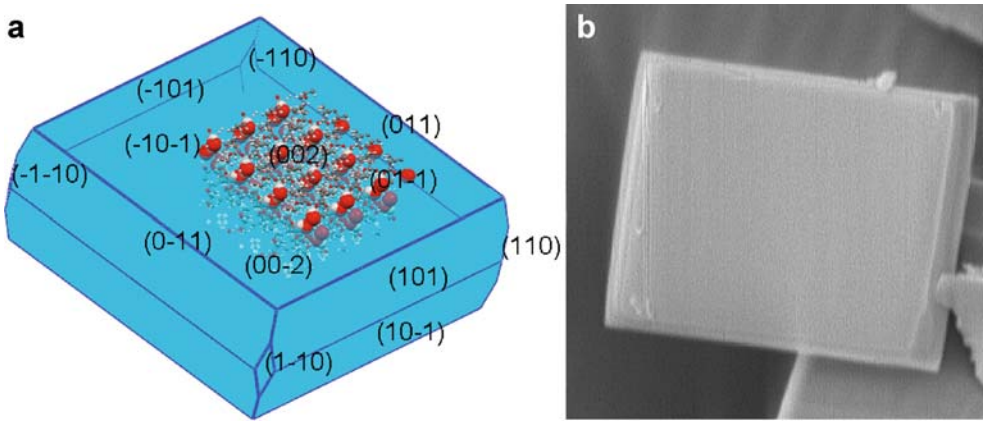

Fig. 4. **a** Erythromycin A dihydrate crystal shape predicted by BFDH model and **b** the observed morphology of L crystals grown in the presence of 0.45 wt.% of HPC

reference. This result suggests a reduced frequency of the (101) planes in the M and H crystals.

EMAD is capable of forming an isomorphic dehydrate (16,25,26). Thus, the water content analysis was performed to verify the hydration state of the model API. According to the results of KF titration, the water content of the additive-modified crystals was 4.5±0.12, 4.2±0.08, and 3.9.±0.16% for L, M, and H crystals, respectively. These values are in agreement with the theoretical water content (4.7%) of EMAD.

Further, possible interactions between the drug and polymer were examined by DSC. The analysis of the DSC thermograms of the samples showed that some melting point depression (by ~2–3°C) and reduction in enthalpies (from 4.5 to 3.4–3.9 J g^{-1}) was a common tendency for the HPC-modified crystals. These reductions in enthalpy of melting may be caused by the presence of amorphous regions in the crystals or by the weakening and disruption of the crystal lattice and order (4). However, no crystalline disorder was detected by PXRD, which does not suggest significant generation of amorphous material. Thus, the peak shifts and enthalpy deviations revealed by DSC may be attributed to interactions between the EMAD crystal surface and the adsorbed additive. Quantitatively, it was approximated that about ~0.2–0.4 wt.% of the polymer may associate with the EMAD crystal faces when the crystallization was performed in the presence of HPC.

Effect of the Additive on Compaction Behavior

The effect of the crystal habit modification on the compactibility of EMAD was evaluated by plotting the crushing strength of powder compacts *vs.* compaction pressure. These data showed that the compaction behavior of the additive-modified crystals was superior to that of either the commercial sample or the reference. In particular, compaction properties of both the commercial sample and the reference were extremely poor, as indicated by severe capping of their compacts in the whole pressure range studied. The compacts produced from the HPC-modified crystals, in contrast, demonstrated a linear relationship between the crushing strength and the compaction force applied, especially in the low pressure range (<5,000 N; Fig. 6a).

DISCUSSION

Molecular Insight into the Nature of Host–Additive Interactions

Considering the general effect of the additives on crystallization kinetics, it can be assumed that with addition of HPC to the crystallization medium the mean growth rate is suppressed and altered growth rates of individual crystal faces result in crystal habit modification. Theoretically, EMAD is expected to grow as plates with the fastest growth along the *b*-axis as this direction has the strongest drug–drug intermolecular interactions (27) and one of the shortest unit cell dimensions (b=9.632 Å). The growth rate along the *a*-axis (a=9.183 Å) should be of the same magnitude since this direction bears drug molecules H-bonded through the water molecules. The morphology of L crystals grown in the presence of 0.45 wt.% of the additive reassembles the BFDH model. Upon increase in the additive concentration, EMAD grows as more elongated crystals, apparently with decreased growth rate along the *b*-axis.

Structural anisotropy of organic crystals, including APIs, gives rise to the substantial differences in surface chemistry of their terminating faces (28,29). In order to reveal the specific functional groups exposed to the dominant crystal faces of EMAD, surface chemistry analysis of these faces was performed using molecular modeling tools (Table I and Fig. 7). This analysis revealed that the largest (002) face of the crystal is likely to be $-N(CH_3)_2$-terminated and thus develops the most hydrophobic crystal face, while the (011) face is the most hydrophilic, with the two water molecules being exposed to this face.

Cellulose derivatives have been previously shown to be capable of interacting with the drug molecules via H-bonds (28,30,31). We assume that the polymer reversibly interacts with the EMAD crystal surfaces, especially with (011) and (101), during crystallization thus suppressing overall crystal growth. Possible interaction sites of HPC with the crystal surface are those where the water molecules are bonded to the drug. Specifically, the hydroxyl groups of HPC may interact with the EMAD surface via the H-bonds O6...HO-HPC,

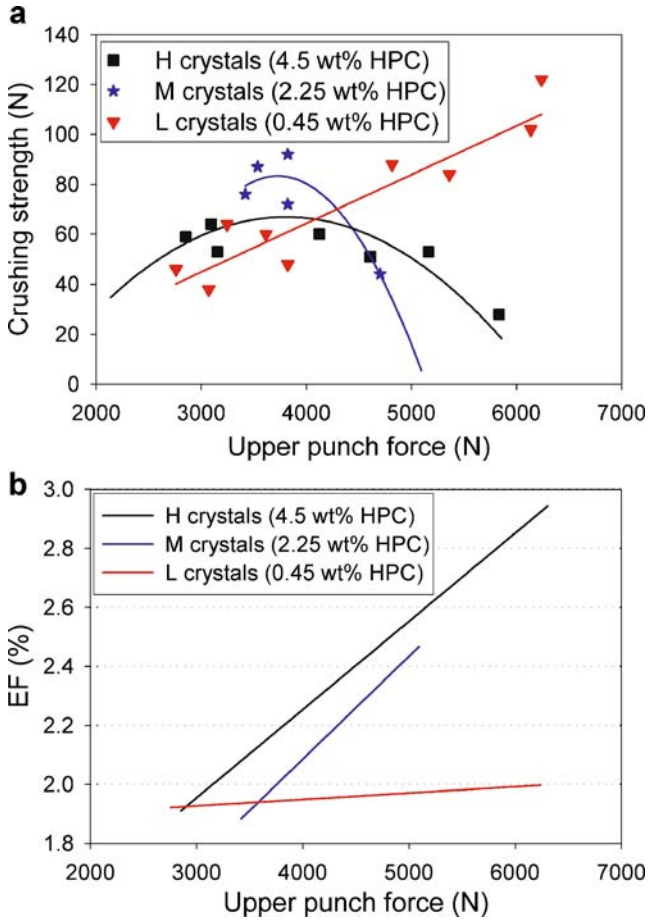

Fig. 6. Tabletting performance of the HPC-modified erythromycin A dihydrate crystals: **a** crushing strength and **b** elasticity factor (*EF*) as functions of compaction force

Table I. Surface Chemistry of the Dominant Crystal Faces of Erythromycin A Dihydrate

Crystal face	Functional groups and water molecules exposed to the face (in numbers)							
(hkl)	–OH	$-C_2H_5$	$-CH_3$	–COC–	$-OCH_3$	$-N(CH_3)_2$	$-(CH_2)$	H_2O
(002)			–	–	–	2	1	–
(011)	2	1	4	3	1	–		2
(101)	1	–	5	1	–	1		1

O12...HO-HPC, or O4H...O-HPC (see Fig. 1a). Clearly, the suppressing effect of an additive on the crystal growth should increase as a function of its concentration in the crystallization medium. At relatively low additive concentrations, this effect is less pronounced due to insufficient number of HPC molecules (or more precisely, specific functional groups) and more equidimensional crystals are produced. As additive concentration increases, more HPC molecules are available and the probability of the host–additive interactions increases. Under these conditions, the preferred adsorption of HPC at the {011} crystal faces leads to retarded crystal growth in the *b* direction and this effect is macroscopically seen as elongated EMAD crystals.

Relationship Between the Crystal Morphology and Tabletability

At the fundamental level, behavior of the material during tablet compression, including capping phenomena, is defined by internal structure of the crystal (8,32,33). At the same time, crystal habit is known to influence compaction profile through its effect on the relative orientation of the crystallites during compression (34,35). Since all the crystals produced in this study had the same solid-state structure, as verified by PXRD, the differences in their compaction behavior can be attributed to the modified crystal habit. In general, less equidimensional crystals (such as M and H crystals) have a tendency to pack preferentially, with their longer dimension(s) oriented normally to the compression axis. This is a possible explanation for producing weak compacts containing M or H crystals at higher compaction pressures (see Fig. 6a). An improved tabletting performance of more equidimensional L crystals is likely due to their random orientation during compression. Furthermore, the additive-induced modification of the crystals was found to alter their elastic properties. In the particular case of L crystals, the improved tabletability correlated with the least and almost constant elastic response within the whole range of compaction forces studied (Fig. 6b). Future studies that will employ various predictive tools (36,37) are, however, needed to relate the crystal habit with tabletting performance of the pharmaceutical materials.

CONCLUSIONS

Crystal morphology engineering proved to be an effective tool for enhancing tabletting performance of pharmaceutical solids. By using pharmaceutically accepted excipients as crystal habit modifiers, toxicity and/or environmental concerns can be overcome. In long-term perspective, this study creates a basis for developing strategies to redefine APIs as a drug substance plus excipient(s) to eventually produce pharmaceutical materials with desirable properties during the bottom-up unit operation such as crystallization, thus avoiding potential problems during further formulation steps.

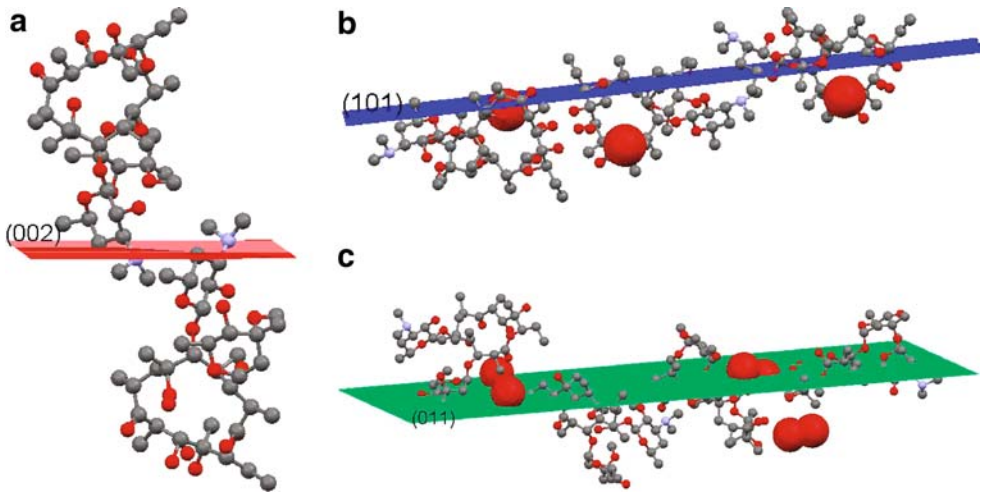

Fig. 7. Structure of the dominant crystal faces (*hkl*) of erythromycin A dihydrate: **a** (002), **b** (101), and **c** (011). The hydrogens are omitted for clarity

ACKNOWLEDGEMENTS

The Finnish Funding Agency for Technology and Innovation (TEKES) is gratefully acknowledged for financial support.

REFERENCES

1. C. R. Gardner, C. T. Walsh, and O. Almarsson. Drugs as materials: valuing physical form in drug discovery. *Nat. Rev. Drug Discov.* **3**:926–934 (2004).
2. P. York. Crystal engineering and particle design for the powder compaction process. *Drug Dev. Ind. Pharm.* **18**:677–721 (1992).
3. N. Blagden, M. de Matas, P. T. Gavan, and P. York. Crystal engineering of active pharmaceutical ingredients to improve solubility and dissolution rates. *Adv. Drug Deliv. Rev.* **59**:617–630 (2007).
4. P. York. Solid-state properties of powders in the formulation and processing of solid dosage forms. *Int. J. Pharm.* **14**:1–28 (1983).
5. S. Datta, and D. J. Grant. Crystal structures of drugs: advances in determination prediction and engineering. *Nat. Rev. Drug Discov.* **3**:42–57 (2004).
6. R. Bandyopadhyay, and D. J. Grant. Influence of crystal habit on the surface free energy and interparticulate bonding of L-lysine monohydrochloride dihydrate. *Pharm. Dev. Technol.* **5**:27–37 (2000).
7. J. T. Carstensen. *Advanced pharmaceutical solids*, Marcel Dekker, New York, 2001.
8. C. Sun, and D. J. Grant. Influence of crystal shape on the tableting performance of L-lysine monohydrochloride dihydrate. *J. Pharm. Sci.* **90**:569–579 (2001).
9. J. K. Haleblian. Characterization of habits and crystalline modification of solids and their pharmaceutical applications. *J. Pharm. Sci.* **64**:1269–1288 (1975).
10. R. J. Davey, J. W. Mullin, and M. J. L. Whiting. Habit modification of succinic acid crystals grown from different solvents. *J. Cryst Growth*. **58**:304–312 (1982).
11. P. V. Marshall, and P. York. Crystallization solvent induced solid-state and particulate modifications of nitrofurantoin. *Int. J. Pharm.* **55**:257–263 (1989).
12. H. A. Garekani, F. Sadeghi, A. Badiee, S. A. Mostafa, and AR Rajabi-Siahboomi. Crystal habit modifications of ibuprofen and their physicomechanical characteristics. *Drug Dev. Ind. Pharm.* **27**:803–809 (2001).
13. S. L. Raghavan, A. Trividic, A. F. Davis, and J. Hadgraft. *Int. J. Pharm.* **212**:213–221 (2001).
14. N. Rodríguez-Hornedo, and D. Murphy. Surfactant-facilitated crystallization of dihydrate carbamazepine during dissolution of anhydrous polymorph. *J. Pharm. Sci.* **93**:449–460 (2004).
15. A. Kuldipkumar, Y. T. F. Tan, M. Goldstein, Y. Nagasaki, G. G. Z. Zhang, and G. S. Kwon. Amphiphilic diblock copolymer as crystal habit modifier. *Cryst Growth Des.* **5**:1781–1785 (2005).
16. S. Mirza, I. Miroshnyk, J. Heinämäki, L. Christiansen, M. Karjalainen, and J. Yliruusi. Influence of solvents on the variety of crystalline forms of erythromycin. *AAPS PharmSci*. **5**2:12 (2003).
17. O. Antikainen, and J. Yliruusi. Determining the compression behavior of pharmaceutical powders from the force-distance compression profile. *Int. J. Pharm.* **252**:253–261 (2003).
18. G. A. Stephenson, J. G. Stowell, P. H. Toma, R. R. Pfeiffer, and S. R. Byrn. Solid-state investigations of erythromycin A dihydrate: structure NMR spectroscopy and hygroscopicity. *J. Pharm. Sci.* **86**:1239–1244 (1997).
19. G. Friedel. Studies on the law of Bravais. *Bull. Soc. Franc. Min.* **30**:326–455 (1907).
20. J. D. H. Donnay, and D. Harker. A new law of crystal morphology extending the law of Bravais. *Am. Mineral.* **22**:446–467 (1937).
21. M. Lang, A. L. Gzesiak, and A. J. Matzger. The use of polymer heteronuclei for crystalline polymorph selection. *J. Am. Chem. Soc.* **124**:14834–14835 (2002).
22. T. Mukuta, A. Y. Lee, T. Kawakami, and A. S. Myerson. Influence of impurities on the solution-mediated phase transformation of an active pharmaceutical ingredient. *Cryst. Growth Des.* **5**:1429–1436 (2005).
23. L.-F. Huang, and W.-Q. Tong. Impact of solid state properties on developability assessment of drug candidates. *Adv. Drug Deliv. Rev.* **56**:321–334 (2004).
24. S. Mirza, J. Heinämäki, I. Miroshnyk, J. Rantanen, L. Christiansen, M. Karjalainen, and J. Yliruusi. Understanding processing-induced phase transformations in erythromycin-PEG 6000 solid dispersions. *J. Pharm. Sci.* **95**:1723–1732 (2006).
25. G. A. Stephenson, E. G. Groleau, R. L. Kleemann, W. Xu, and D. R. Rigsbee. Formation of isomorphic desolvates: creating a molecular vacuum. *J. Pharm. Sci.* **87**:536–542 (1998).
26. I. Miroshnyk, L. Khriachtchev, S. Mirza, J. Rantanen, J. Heinämäki, and J. Yliruusi. *Cryst Growth Des.* **6**:369–374 (2006).
27. I. Miroshnyk, S. Mirza, P. M. Zorkii, A. E. Obodovskaya, J. Heinämäki, and J. Yliruusi. Interpretation of pharmacokinetic properties of erythromycin and its derivatives on the basis of calculation of intermolecular interaction energy in crystals. *AAPSPharmSci.* **3**(S1) (2001).
28. F. Tian, N. Sandler, K. C. Gordon, C. M. McGoverin, A. Reay, C. J. Strachan, D. J. Saville, and T. Rades. Visualizing the conversion of carbamazepine in aqueous suspension with and without the presence of excipients: a single crystal study using SEM and Raman microscopy. *Eur. J. Pharm. Biopharm.* **64**:326–335 (2006).
29. J. Y. Y. Heng, A. Bismarck, and D. R. Williams. Anisotropic surface chemistry of crystalline pharmaceutical solids. *AAPS PharmSciTech.* **7**(4) (2006).
30. I. Katzhendler, R. Azoury, and M. Friedman. Crystalline properties of carbamazepine in sustained release hydrophilic matrix tablet based on hydroxypropyl methylcellulose. *J. Control Release*. **54**:69–85 (1998).
31. H. Wen, K. R. Morris, and K. J. Park. Hydrogen bonding interactions between adsorbed polymer molecules and crystal surface of acetaminophen. *J. Colloid Interface Sci.* **290**:325–335 (2005).
32. R. J. Roberts, R. C. Rowe, and P. York. The relationship between the fracture properties, tensile strength, and critical stress intensity factor of organic solids and their molecular structure. *Int. J. Pharm.* **125**:157–162 (1995).
33. Y. Feng, and D. J. Grant. Influence of crystal structure on the compaction properties of *n*-alkyl 4-hydroxybenzoate esters (parabens). *Pharm. Res.* **23**:1608–1616 (2006).
34. J. W. Shell. X-ray and crystallographic applications in pharmaceutical research. III. Crystal habit quantitation. *J. Pharm. Sci.* **52**:100–101 (1963).
35. R. Bandyopadhyay, and D. J. Grant. Plasticity and slip system of plate-shaped crystals of L-lysine monohydrochloride dihydrate. *Pharm. Res.* **19**:491–496 (2002).
36. A. P. Plumb, R. C. Rowe, P. York, and M. Brown. Optimisation of the predictive ability of artificial neural network (ANN) models: a comparison of three ANN programs and four classes of training algorithm. *Eur. J. Pharm. Sci.* **25**:395–405 (2005).
37. Q. Shao, R. C. Rowe, and P. York. Comparison of neurofuzzy logic and decision trees in discovering knowledge from experimental data of an immediate release tablet formulation. *Eur. J. Pharm. Sci.* **31**:129–136 (2007).